Physica A xx (xxxx) xxx–xxx

Contents lists available at ScienceDirect

Physica A

journal homepage: www.elsevier.com/locate/physa

Characterizing cerebrovascular dynamics with the wavelet-based multifractal formalism

Q1 A.N. Pavlov [a,b,*], A.S. Abdurashitov [a], O.A. Sindeeva [c], S.S. Sindeev [c], O.N. Pavlova [a], G.M. Shihalov [a], O.V. Semyachkina-Glushkovskaya [c]

[a] Department of Physics, Saratov State University, Astrakhanskaya Str. 83, 410012, Saratov, Russia
[b] Saratov State Technical University, Politechnicheskaya Str. 77, 410054, Saratov, Russia
[c] Department of Biology, Saratov State University, Astrakhanskaya Str. 83, 410012, Saratov, Russia

HIGHLIGHTS

- We reveal responses of cerebral circulations to changed peripheral blood pressure.
- We show different reactions in the dynamics of large and small cerebral vessels.
- Complexity of the microcerebral dynamics increases with peripheral blood pressure.

ARTICLE INFO

Article history:
Received 3 May 2015
Received in revised form 1 September 2015
Available online xxxx

Keywords:
Multifractality
Wavelet transform
Cerebrovascular dynamics
Laser speckle contrast imaging

ABSTRACT

Using the wavelet-transform modulus maxima (WTMM) approach we study the dynamics of cerebral blood flow (CBF) in rats aiming to reveal responses of macro- and microcerebral circulations to changes in the peripheral blood pressure. We show that the wavelet-based multifractal formalism allows quantifying essentially different reactions in the CBF-dynamics at the level of large and small cerebral vessels. We conclude that unlike the macrocirculation that is nearly insensitive to increased peripheral blood pressure, the microcirculation is characterized by essential changes of the CBF-complexity.

1. Introduction

Multiscale characterization of various natural systems was the subject of many studies performed during the last years (e.g., Refs. [1–9]). The wavelet-based multifractal formalism recently proposed by Muzy et al. [10–12] provided a way of Q2 statistical analysis of essentially nonstationary and inhomogeneous processes. This tool outperforms the earlier elaborated structure function method [13] that does not allow characterizing full range of singularities due to fundamental drawbacks. Thus, the structure function approach leads to divergences when analyzing weak singularities (small fluctuations) in experimental data. It does not allow characterizing singularities in derivatives of the analyzed signal thus restricting the range of the Hölder exponents by 1. The WTMM approach [10–12] possesses essential advantages in both, ability of characterizing a wider range of scaling characteristics, and stability of estimating the singularity spectrum. This tool has demonstrated its essential potential in solving different diagnostic problems by revealing small changes of signals structure being not distinguished with the standard data processing techniques [7,8,14–16].

* Corresponding author at: Department of Physics, Saratov State University, Astrakhanskaya Str. 83, 410012, Saratov, Russia.
E-mail address: pavlov.lesha@gmail.com (A.N. Pavlov).

http://dx.doi.org/10.1016/j.physa.2015.09.007
0378-4371/

A promising field of application of the wavelet-based multifractal formalism is the characterizing of cerebrovascular dynamics where advanced data processing tools could provide informative markers of early stages of transformations of normal physiological processes into pathological dynamics. Noninvasive analysis of cerebral blood flow is typically provided with optical coherent-domain methods such as, e.g., the laser speckle contrast imaging (LSCI) [17–19] that possesses a high spatio-temporal resolution. CBF-dynamics is quantified from variations of the speckle pattern that is formed due to the scattering of the coherent light from moving particles of the blood. Temporal changes of the contrast are recalculated into the CBF-velocity.

In this work, based on LSCI-data we analyze responses of the cerebrovascular dynamics in rats to a pharmacological increase in the peripheral blood pressure. An importance of this study is caused by a high risk for the stroke because the hypertension-related disturbances of the cerebral autoregulation are a key reason for the critical changes in CBF associated with this disease [20]. CBF in humans is independent of changes in arterial blood pressure within a range of 60–150 mm Hg and this has become the traditionally accepted model for static cerebral autoregulation [21]. However, clinical and experimental researches conducted over the last several years suggested that systemic hypertension is associated with a high risk for the stroke due to pathological changes in regulatory mechanisms of CBF [22–24]. Therefore, a study of pathophysiological processes contributing increased CBF-sensitivity to peripheral pressure variations may provide a deeper understanding of mechanisms underlying the development of the stroke.

The paper is organized as follows. In Section 2 we describe experimental techniques and methods used for data processing. Analysis of abilities of the WTMM-approach in quantifying the hypertension-related disturbances of the cerebral autoregulation at the levels of macro- and microcirculation is performed in Section 3. Section 4 contains some concluding remarks.

2. Experiments and methods

2.1. Experimental procedure

Experiments were performed in mongrel normotensive male rats ($n = 12$) weighing from 200 to 250 g in accordance with the Guide for the Care and Use of Laboratory Animals published by the US National Institutes of Health [25]. To study changes in the CBF-dynamics caused by increased arterial blood pressure, we performed a pharmacological test using the phenylephrine. Phenylephrine does not cross the blood–brain barrier [26] and, therefore, there is an ability of studying reactions of CBF induced by the phenylephrine-related acute peripheral hypertension.

One day before the experiment, rats were instrumented with polyethylene catheters for monitoring mean arterial pressure (MAP). For implantation of catheters, rats were anesthetized with ketamine (40 mg/kg, ip) supplemented with xylazine (5 mg/kg, ip). The polyethylene catheter (PE-50 with a PE-10 tip, Scientific Commodities INC., Lake Havasu City, Arizona) was inserted into the femoral artery. In addition, the femoral vein was catheterized with PE-50 tubing fused PE-10 for phenylephrine infusion. MAP was recorded in the home cages of conscious, unrestrained rats. Blood pressure signals were acquired with the PowerLab system (ADInstruments, Australia) using a pressure transducer.

When performing the base-line measurement, MAP was recorded continuously during 30 min after the phenylephrine injections in different doses (dose 1: 0.125 μg/kg, iv, and dose 2: 0.25 μg/kg, iv). The time and the magnitude of pressure responses to increased doses of phenylephrine were controlled in each rat. Generally, the phenylephrine injections increased the arterial blood pressure by about 10%. The craniotomy was done in anesthetized rats using the dental drill (Mikroton, Aesculap) with a constant saline irrigation to prevent tissue overheating. Measuring of CBF in rat cortex was performed 30 min after the surgery in order to CBF becomes stable. Q3

2.2. Laser speckle contrast imaging

Monitoring of CBF was provided with a home-made system for laser speckle contrast imaging (LSCI). Speckle images were recorded as follows: the exposed rat cortex was illuminated by the HeNe laser (Thorlabs HNL210L, 632.8 nm). Raw laser speckle images were acquired with the monochromatic CMOS camera Basler acA2500-14 gm and Computar M1614-MP2 lens. The rate of image recording was set to 40 frames/second. Noise was reduced in the course of time averaging over 50 images using a moving window (55 × 55 pixels). The Gaussian approach was used to convert the speckle contrast data into flow velocity signals. Dynamical features of CBF characterizing the venous (the sagittal sinus) and microcerebral (small cerebral vessels of microcirculatory network) circulation were studied in normal state and after each dose of the phenylephrine injection.

2.3. WTMM-approach

Analysis of CBF-velocity was performed with the WTMM-method proposed by Muzy et al. [10] that is described in detail in the review paper [12]. It is based on the continuous wavelet-transform of a function $f(x)$

$$T(s,z) = \frac{1}{\sqrt{s}} \int_{-\infty}^{\infty} f(x)\psi\left(\frac{x-z}{s}\right) \mathrm{d}x, \tag{1}$$

Please cite this article in press as: A.N. Pavlov, et al., Characterizing cerebrovascular dynamics with the wavelet-based multifractal formalism, Physica A (2015), http://dx.doi.org/10.1016/j.physa.2015.09.007

where the parameters s and z define the scale and the translation of the wavelet ψ. Singularities of the function $f(x)$ are typically studied with real-valued wavelets ψ such as, e.g., WAVE

$$\psi = x \exp\left(-\frac{x^2}{2}\right) \tag{2}$$

or MHAT

$$\psi = (1 - x^2) \exp\left(-\frac{x^2}{2}\right) \tag{3}$$

representing the first and the second derivatives of the Gaussian function, respectively, although higher derivatives can also be applied.

Let us consider the function $f(x)$ that is n (but not $n + 1$) times differentiable at a point $x = z^*$. Such function can be expanded into the Taylor series $P_n(x)$ up to nth degree. The Hölder exponent is defined as the maximal value of h satisfying the condition

$$|f(x) - P_n(x - z^*)| \leq C|x - z^*|^h. \tag{4}$$

In the vicinity of a singularity, the function $f(x)$ represents a sum of a regular ($P_n(x)$) and an irregular ($C|x - z^*|^h$) part

$$f(x) = P_n(x - z^*) + C|x - z^*|^h. \tag{5}$$

If the wavelet ψ has m vanishing moments

$$\int_{-\infty}^{\infty} x^m \psi(x) \mathrm{d}x = 0, \tag{6}$$

then the polynomial trend $P_n(x)$ for $n \leq m$ is ignored

$$\int_{-\infty}^{\infty} P_n(x) \psi(x) \mathrm{d}x = 0 \tag{7}$$

and, therefore, the wavelet-transform of the function $f(x)$ near the considered singularity can be written as

$$T(s, z^*) = C\sqrt{s} \int_{-\infty}^{\infty} \psi(x) |sx|^{h(z^*)} \mathrm{d}x. \tag{8}$$

Aiming to deal with a simpler power-law dependence of wavelet-coefficients from the scale s, the normalizing factor $1/\sqrt{s}$ in (1) is changed by $1/s$ [12]

$$T(s, z) = \frac{1}{s} \int_{-\infty}^{\infty} f(x) \psi\left(\frac{x - z}{s}\right) \mathrm{d}x. \tag{9}$$

As a result, scaling features of the wavelet-transform coefficients near the singularity point z^*

$$T(s, z^*) \sim s^{h(z^*)}, \quad s \to 0^+ \tag{10}$$

allow easy estimation of the Hölder exponent $h(z^*)$. It is important to mention that the value of h does not depend on the selected wavelet ψ.

If the function $f(x)$ is regular at the point z^*, a significantly faster convergence of $T(s, z^*)$ with s is observed

$$T(s, z^*) \sim s^m, \quad s \to 0^+. \tag{11}$$

Thus, a slower decrease of wavelet-coefficients with the appearance of a skeleton line [12] is a sign of a singular behavior at $x = z^*$.

After performing the wavelet-transform (9), all skeleton lines are extracted representing the lines of local maxima and minima of the wavelet-transform coefficients $T(s, z)$ estimated at fixed values of the scale parameter s. Although the power-law dependence (10) allows computing the Hölder exponent h by defining the slope of the line in the double logarithmic plot ($\log T$ *vs.* $\log s$), this approach is highly unstable and typically leads to incorrect results caused, e.g., by the presence of neighboring singularities that influence each other when the scale s is varied.

Due to this, statistical analysis of singularities is performed using the partition functions $Z(q, a)$ defined as

$$Z(q, s) = \sum_{l \in L(s)} |T(s, z_l(s))|^q, \tag{12}$$

where $L(s)$ denotes a full set of skeleton lines whose points can be treated as maxima of modulus of the wavelet coefficients detected at the scale s, and $z_l(s)$ is the position of the maximum related to the line l. By taking the values $|T(s, z)|$, the stability of the performed analysis increases as compared with the case of $T(s, z)$.

Please cite this article in press as: A.N. Pavlov, et al., Characterizing cerebrovascular dynamics with the wavelet-based multifractal formalism, Physica A (2015), http://dx.doi.org/10.1016/j.physa.2015.09.007

Because $T(s, z)$ can take zero values, $Z(q, s)$ is incorrectly determined at the corresponding parameters (s, z) for $q < 0$. Due to this, the partition functions are estimated as follows

$$Z(q, s) = \sum_{l \in L(s)} \left(\sup_{s' \le s} |T(s', z_l(s'))| \right)^q \sim s^{\tau(q)}. \tag{13}$$

Scaling exponents $\tau(q)$ are computed as slopes of the dependencies $\log Z(q, s)$ *vs.* $\log s$ for each value of q. Finally, the Hölder exponents $h(q)$ and the singularity spectrum $D(h)$ are estimated as

$$h(q) = \frac{\mathrm{d}\tau(q)}{\mathrm{d}q}, \tag{14}$$

$$D(h) = qh - \tau(q). \tag{15}$$

The function $D(h)$ quantifies the Hausdorff dimension D of a subset of points satisfying to the condition $h(x) = h$. The width of the singularity spectrum

$$\Delta_h = h_{\max} - h_{\min}, \tag{16}$$

where $h_{\max}$ and $h_{\min}$ are the maximal and the minimal values of the Hölder exponents, may be treated as a complexity measure that quantifies the range of $h(q)$ describing scaling features of analyzed processes. Simple (the monofractal) processes such as, e.g., $1/f$-noise are described by the singularity spectrum consisting of a single point and $\Delta_h = 0$. Increased complexity is associated with larger values of Δ_h.

The Hölder exponent $h(0)$ typically takes the value similar to the scaling exponent of the detrended fluctuation analysis (DFA) [27,28]. The algorithm of DFA is simpler compared with the WTMM-technique although it can provide analogous characterization of scaling features of complex dynamics [14]. From our experience, the WTMM-method has advantages in processing short data series [29] and in resolving intermediate values of scaling characteristics.

3. Results and discussion

Cerebrovascular dynamics is characterized by a clearly expressed multiscale structure at both, the macroscopic level of large arteries and veins, and the microscopic level of small vessels. Analysis performed in the given work has revealed essentially different reactions of macro- and microcerebral circulation to the phenylephrine-related acute peripheral hypertension.

According to the existing physiological knowledge about the presence of protective mechanisms in the cerebral autoregulation against variations of the peripheral blood pressure, it is expected that cerebral vessels demonstrate subtle signs of possible reactions in the CBF dynamics when the peripheral blood pressure is changed. Analysis of the CBF velocity in the sagittal sinus confirms this assumption. Following Fig. 1, the spectrum of scaling exponents $\tau(q)$ does not demonstrate essential distinctions between different physiological conditions. Despite some variability of $\tau(q)$ that is typical for a normal physiological regulation due to nonstationarity of analyzed processes, all dependencies in Fig. 1(a) verify that the CBF-dynamics is related to multifractal processes since $\tau(q)$ is clearly different from a straight line. The Hölder exponents $h(q)$ show essential variations (Δ_h takes the value near 1.0) thus confirming the conclusion about the multiscale dynamics of CBF (Fig. 1(b)). Nevertheless, there is no distinction between singularity spectra associated with different physiological states (Fig. 1(c)). Thus, we can conclude about small variations of multiscale properties of CBF in normal conditions and under the pharmacologically induced changes in the peripheral blood pressure.

In Fig. 1 we demonstrated quite typical results for the cerebral macrocirculation. Analysis of microcirculation in small cerebral vessels in the same rat showed a quite different response (Fig. 2). By analogy with Fig. 1(a), scaling exponents $\tau(q)$ demonstrate nonlinear dependencies from q thus confirming the presence of multiscale structure of CBF velocity signals at the microscopic level (Fig. 2(a)). The latter is verified by the Hölder exponents $h(q)$ that again show essential variations depending from q. We can see, however, that the range of $h(q)$ is increased after the phenylephrine-related acute peripheral hypertension quantifying a less "homogeneous" structure of the analyzed data (Fig. 2(b), squares). This is also confirmed by a wider singularity spectrum $D(h)$ shown in Fig. 2(c) for the second dose of phenylephrine. Such changes of singularity spectra are associated with increased complexity of the flow dynamics. Complexity measures provide informative characterization of transformation of normal physiological processes into pathological dynamics. Thus, a reduced complexity of the heart rate predicts mortality in patients with head and torso trauma [30]. Complexity of heartbeat variability predicts an outcome in intensive care unit admitted patients with an acute stroke [31].

Q4 The obtained results allow us concluding about different responses in the cerebral macro- and microcirculation. This conclusion is confirmed by statistical analysis performed for all animals. Taking into account that mean Hölder exponent and, therefore, the position of the maximum of $D(h)$ show essential distinctions between rats, we normalized the width of $D(h)$ for each animal by the corresponding value at a normal condition (the "control" state). The obtained results are given in Fig. 3 as mean values ± SE. They illustrate obvious differences between macroscopic and microscopic cerebral dynamics (dose 1: 0.96 ± 0.12 *vs.* 1.67 ± 0.41, dose 2: 1.02 ± 0.06 *vs.* 1.59 ± 0.30, respectively). The Mann–Whitney test confirms significant distinctions in the microscopic cerebral dynamics after the phenylephrine injections compared with the control group (dose 1: $p = 0.012$, dose 2: $p = 0.016$).

Please cite this article in press as: A.N. Pavlov, et al., Characterizing cerebrovascular dynamics with the wavelet-based multifractal formalism, Physica A (2015), http://dx.doi.org/10.1016/j.physa.2015.09.007

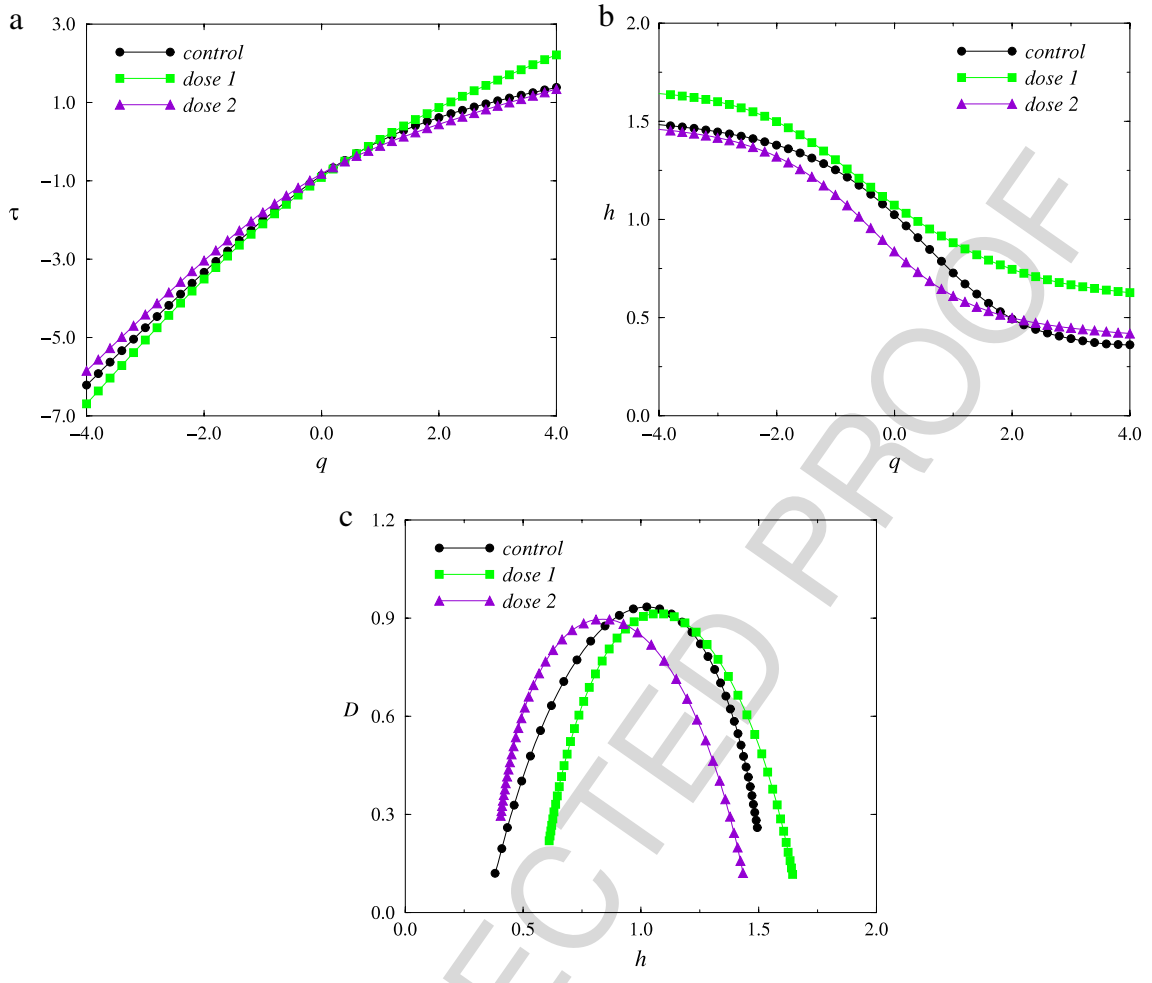

Fig. 1. Multifractal analysis of CBF-dynamics in a rat studied at the macroscopic level of the sagittal sinus: (a) the scaling exponents $\tau(q)$, (b) the Hölder exponents $h(q)$, and (c) the singularity spectra $D(h)$.

4. Conclusions

The wavelet-based multifractal formalism is probably the most powerful tool for statistical analysis of nonstationary and inhomogeneous processes. Besides, this approach has demonstrated its essential potential is quantifying complex dynamics of natural systems from short and noisy data [16] that is important when studying dynamics of living systems. Due to adaptation processes, extracting information about changes in regulatory mechanisms and their time-varying responses should be performed from a quite limited amount of data. Reactions of CBF-dynamics considered in this work represent an example of such limitations. The most pronounced changes in the peripheral blood pressure after the phenylephrine injection may take about 2–3 min and, therefore, quantifying responses in the CBF-dynamics should be provided based on short data series. The WTMM-approach has advantages over many standard data processing tools. In particular, it demonstrates a faster convergence with the amount of data compared with the correlation analysis [29].

Based on the WTMM-approach we studied the problem of characterizing CBF-dynamics in rats when the peripheral blood pressure increases. Although it is expected that the cerebral circulation is insensitive to such variations of the peripheral blood pressure, we have found that responses in the CBF-dynamics are essentially different at the macroscopic level of the sagittal vein and the microscopic level of small cerebral vessels of the microcirculatory network. The macrocirculation is nearly independent of changes in the peripheral blood pressure while the microcirculation is characterized by a significant increase in the complexity. As a complexity measure we used the width of the singularity spectrum that represents a measure of "inhomogeneity" of the analyzed experimental data. The obtained results allow us concluding that physiological assumptions about a static cerebral autoregulation need revisions for vessels of microcirculatory network. We can also conclude that the WTMM-approach can be considered as a promising tool for providing a deeper understanding of mechanisms underlying the transition of normal physiological processes in the cerebral autoregulation into pathological dynamics.

Please cite this article in press as: A.N. Pavlov, et al., Characterizing cerebrovascular dynamics with the wavelet-based multifractal formalism, Physica A (2015), http://dx.doi.org/10.1016/j.physa.2015.09.007

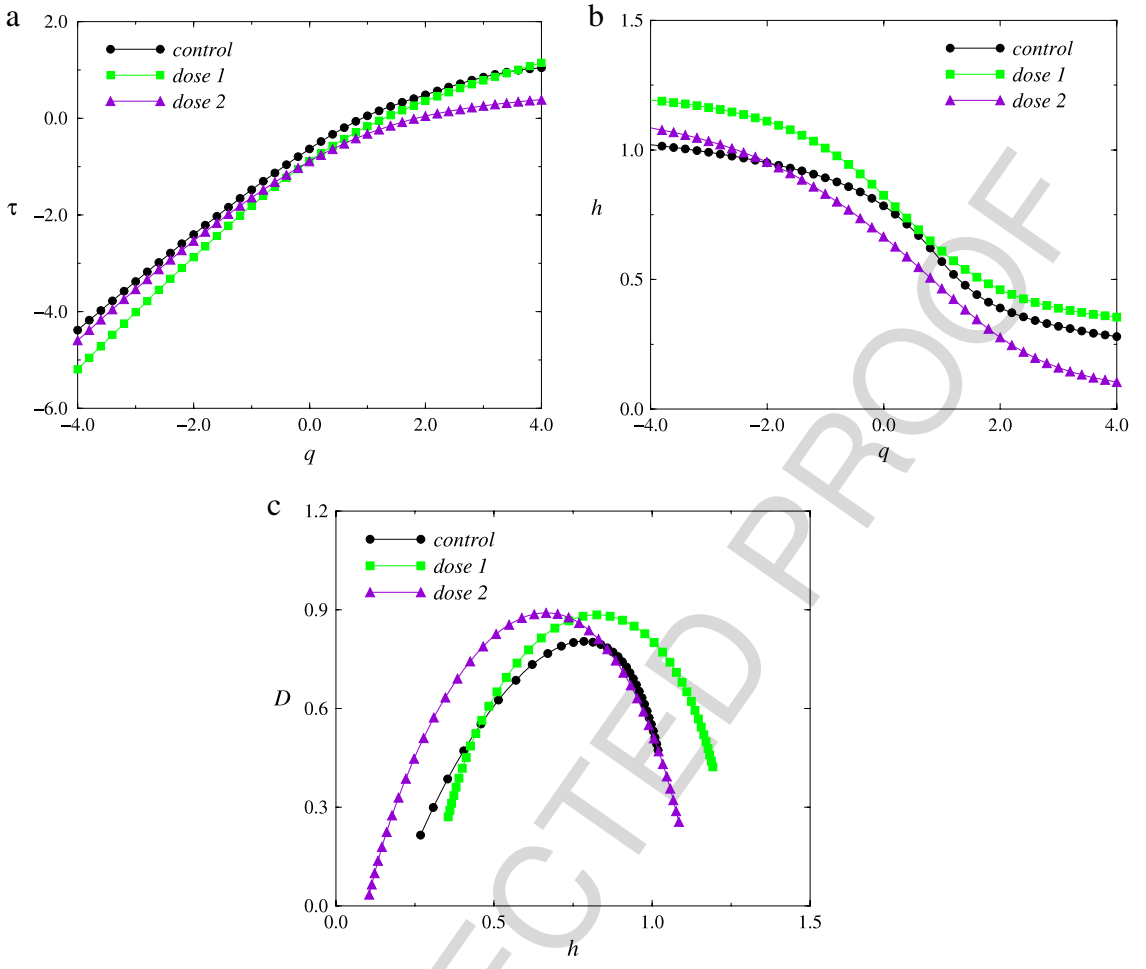

Fig. 2. Multifractal analysis of CBF-dynamics in a rat studied at the microscopic level of small vessels: (a) the scaling exponents $\tau(q)$, (b) the Hölder exponents $h(q)$, and (c) the singularity spectra $D(h)$.

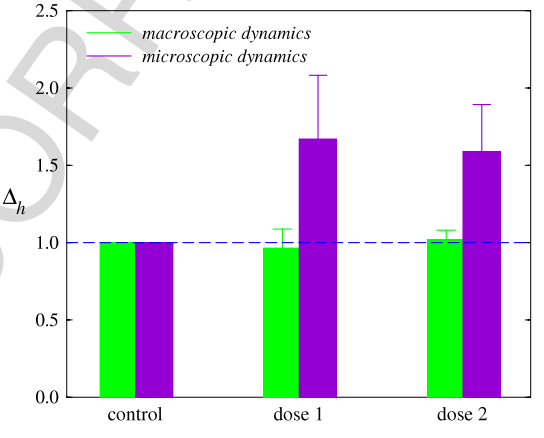

Fig. 3. Distinctions in responses of macroscopic and microscopic cerebral dynamics to the phenylephrine-related increases in the peripheral blood pressure.

Acknowledgment

This work was supported by the Russian Science Foundation (Agreement 14-15-00128).

Please cite this article in press as: A.N. Pavlov, et al., Characterizing cerebrovascular dynamics with the wavelet-based multifractal formalism, Physica A (2015), http://dx.doi.org/10.1016/j.physa.2015.09.007

References

[1] A. Bunde, S. Havlin (Eds.), Fractals in Science, Springer, Berlin, 1994.
[2] B.B. Mandelbrot, Multifractals anf 1/F Noise: Wild Self-Affinity in Physics, Springer-Verlag, New York, 1999.
[3] R. Benzi, L. Biferale, G. Paladin, A. Vulpiani, M. Vergassola, Phys. Rev. Lett. 67 (1991) 2299.
[4] B.J. Strait, T.G. Dewey, Phys. Rev. E 52 (1995) 6588.
[5] J. Arrault, A. Arneodo, A. Davis, A. Marshak, Phys. Rev. Lett. 79 (1997) 75.
[6] V. Afraimovich, G.M. Zaslavsky, Phys. Rev. E 55 (1997) 5418.
[7] P.Ch. Ivanov, L.A.N. Amaral, A.L. Goldberger, S. Havlin, M.G. Rosenblum, Z.R. Struzik, H.E. Stanley, Nature 399 (1999) 461.
[8] H.E. Stanley, L.A.N. Amaral, A.L. Goldberger, S. Havlin, P.Ch. Ivanov, C.-K. Peng, Physica A 270 (1999) 309.
[9] A. Arneodo, N. Decoster, S.G. Roux, Phys. Rev. Lett. 83 (1999) 1255.
[10] J.F. Muzy, E. Bacry, A. Arneodo, Phys. Rev. Lett. 67 (1991) 3515.
[11] J.F. Muzy, E. Bacry, A. Arneodo, Phys. Rev. E 47 (1993) 875.
[12] J.F. Muzy, E. Bacry, A. Arneodo, Int. J. Bifurcation Chaos 4 (1994) 245.
[13] U. Frish, G. Parisi, in: M. Ghil, R. Benzi, G. Parisi (Eds.), Turbulence and Predictability in Geophysical Fluid Dynamics and Climate Dynamics, North-Holland, Amsterdam, 1985, p. 71.
[14] A.N. Pavlov, O.V. Sosnovtseva, A.R. Ziganshin, N.-H. Holstein-Rathlou, E. Mosekilde, Physica A 316 (2002) 233.
[15] A.N. Pavlov, A.R. Ziganshin, O.A. Klimova, Chaos Solitons Fractals 24 (2005) 57.
[16] A.N. Pavlov, V.S. Anishchenko, Phys. Usp. 50 (2007) 819.
[17] J.D. Briers, S. Webster, J. Biomed. Opt. 1 (1996) 174.
[18] S. Liu, P. Li, Q. Luo, Opt. Express 16 (2008) 14321.
[19] D.A. Boas, A.K. Dunn, J. Biomed. Opt. 15 (2010) 011109.
[20] B.B. Johansson, Clin. Exp. Pharmacol. Physiol. 26 (1999) 563.
[21] N.A. Lassen, Physiol. Rev. 39 (1959) 183.
[22] L.L. Beason-Held, A. Moghekar, A.B. Zonderman, M.A. Kraut, S.M. Resnick, Stroke 39 (2007) 1766.
[23] P.J. Gianaros, S.W. Derbyshire, J.C. May, et al., Psychophysiology 42 (2005) 627.
[24] P.J. Gianaros, P.J. Greer, C.M. Ryan, Neuroimage 31 (2006) 754.
[25] Guide for the Care and Use of Laboratory Animals, eighth ed., The National Academies Press, Washington, 2011, http://oacu.od.nih.gov/regs/guide/guide.pdf.
[26] J. Olesen, Neurology 22 (1972) 978.
[27] C.-K. Peng, S. Havlin, H. Stanley, A. Goldberger, Chaos 5 (1995) 82.
[28] S. Havlin, S. Buldyrev, A. Bunde, A. Goldberger, P. Ivanov, C.-K. Peng, H. Stanley, Physica A 273 (1999) 46.
[29] A.N. Pavlov, O.N. Pavlova, Tech. Phys. Lett. 34 (2008) 306.
[30] W.P. Riordan Jr., P.R. Norris, J.M. Jenkins, J.A. Morris Jr., J. Surg. Res. 156 (2) (2009) 283.
[31] S.C. Tang, H.I. Jen, Y.H. Lin, C.S. Hung, W.J. Jou, P.W. Huang, J.S. Shieh, Y.L. Ho, D.M. Lai, A.Y. Wu, J.S. Jeng, M.F. Chen, J. Neurol. Neurosurg. Psychiatry 86 (1) (2015) 95.

Please cite this article in press as: A.N. Pavlov, et al., Characterizing cerebrovascular dynamics with the wavelet-based multifractal formalism, Physica A (2015), http://dx.doi.org/10.1016/j.physa.2015.09.007